Available at www.sciencedirect.com

SCIENCE DIRECT®

journal homepage: www.elsevier.com/locate/watres

Development of a tubular high-density plasma reactor for water treatment

Derek C. Johnson[a], *David S. Dandy*[a,*], *Vasgen A. Shamamian*[b]

[a]*Department of Chemical & Biological Engineering, Colorado State University, Fort Collins, CO 80523, USA*
[b]*Dow Corning Corporation, Auburn, MI 48611, USA*

ARTICLE INFO

Article history:
Received 25 April 2005
Received in revised form
9 November 2005
Accepted 10 November 2005

Keywords:
Reaction kinetics
Tubular high-density plasma reactor
MTBE
BTEX

ABSTRACT

Experiments have yielded a number of important insights into the energy distribution, sparging and oxidation of methyl *tert*-butyl ether (MTBE), benzene, ethylbenzene, toluene, *m*- and *p*-xylene, and *o*-xylene (BTEX) in a dense medium plasma reactor (DMPR). It has been found that the DMPR transferred a relatively small amount of electrical energy, approximately 4% in the form of sensible heat, to the surrounding bulk liquid. Rate constants associated with plasma initiated oxidation, interphase mass transfer and photolysis were determined using a combination of non-linear least squares analysis and MATLAB® optimization for each species. The rate constants developed for the DMPR, in conjunction with a species mass balance on a prototype tubular high-density plasma reactor, have been applied to determine the removal rates of MTBE and the BTEXs when operating in batch and continuous flow configurations. The dependence of contaminant concentration on parameters such as treatment time, the number of pin electrodes, electrode gap, and volumetric flow rate has been determined. It was found that, under various design specifications and operating conditions, the tubular high-density plasma reactor may be an effective tool for the removal of volatile organic compounds from aqueous solutions.

1. Introduction

Plasma treatment of contaminated water appears to be a promising alternative for the oxidation of aqueous organic pollutants. A discussion of reactor configurations employing both thermal and non-thermal plasma reported in the literature is included as Supplementary Materials. This work, however, is focused on the dense medium plasma reactor (DMPR) illustrated in Fig. 1. The DMPR was developed by Denes and coworkers (Denes and Young, 1996) to react liquid/vapor phase species in an induced plasma state using low-temperature plasma chemistry. The DMPR has been investigated as a tool for the disinfection of microbial contaminated water. Experiments conducted by Manolache et al. (2001) focused on quantifying the inactivation of specific bacteria and the mechanisms within the DMPR responsible for the disinfection. Water was artificially contaminated with 16 Gram-positive and Gram-negative bacterial species. To reduce the voltage required to initiate a plasma discharge, oxygen or argon was bubbled through the plasma zone. With 20 s of argon plasma treatment, 91% of the colony forming units (cfu) per mL of solution were either inactivated or destroyed. This increased to greater than 98% when the solution was treated for 60 s. The results were slightly better with an oxygen plasma treatment. After 20 s, 98.8% of the cfu/mL were disinfected, with only a slight increase of 0.13% and 0.53% for an additional 40 and 100 s of treatment, respectively. The

*Corresponding author. Tel.: +1 970 491 7437; fax: +1 970 491 7369.
E-mail address: dandy@colostate.edu (D.S. Dandy).
0043-1354/$ - see front matter © 2005 Elsevier Ltd. All rights reserved.
doi:10.1016/j.watres.2005.11.015

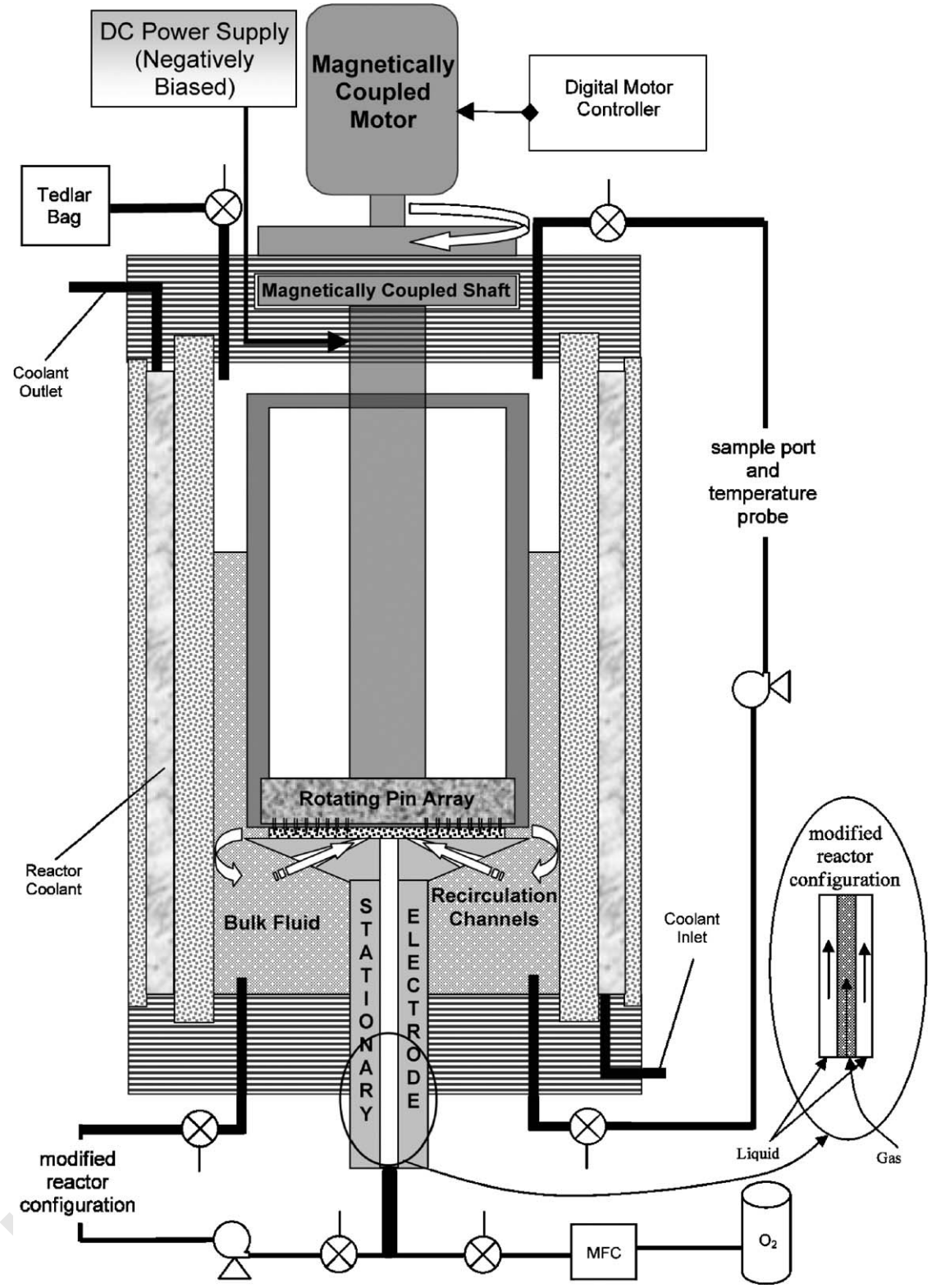

Figure 1 – A schematic of the DMPR and a modified reactor configuration implemented by Johnson et al. (2003). A more detailed description of the reactor can be found in Manolache et al. (2001, 2004).

additional disinfection capability of the oxygen plasma can be attributed to the formation of ozone, a powerful disinfectant.

The oxidation of methyl *tert*-butyl ether (MTBE) and formation of oxidation products in a DMPR have also been explored (Johnson et al., 2003). It was found that carbon dioxide was formed due to electron-impact dissociation reactions in the oxygen plasma, while acetone, *tert*-butyl formate and formaldehyde were formed as a result of

oxidation initiated by species formed due to the plasma discharge. To determine the effect of increased volumetric flow rate of the bulk solution through the plasma on the reaction rate, a modification was made to the original reactor. As illustrated in Fig. 1, the center shaft in the stationary electrode was modified to create an annulus in which oxygen passed through the center and the aqueous solution flowed through the outer annular ring. To compare the rate constants for MTBE removal between the original DMPR and the modified reactor, a pseudo first-order rate equation was developed. It was found that the rate constant associated with the modified reactor was approximately 33% higher than that of the original reactor.

The DMPR has also been used to oxidize aqueous aromatic organic pollutants (Manolache et al., 2004). Distilled water was contaminated with benzene, toluene, ethylbenzene, *m*- and *p*-xylene, and *o*-xylene (BTEX), with initial concentrations ranging from 194 to 860 ppm. Five experiments were performed to quantify the effects of varying the oxygen flow rate and current on the removal of the organic species from solution. Of the compounds examined, benzene was found to be the most difficult species to remove. It was observed that the attenuation of all compounds depended strongly on the current intensity and oxygen flow rate (Manolache et al., 2004). However, this dependence was not monotonic across the range of current values and gas flow rates tested. As a result, Manolache et al. (2004) proposed that an optimal condition exists for the oxidation of the aromatic compounds that did not necessarily correspond to the highest current and oxygen flow rate.

While the oxidation and disinfection experiments performed in a DMPR have shown promising results, the solution volume that can be treated in the reactor is quite small. This is due to the small plasma volume generated from each pin electrode and the fact that the oxidation chemistry is performed in the plasma and/or in the vicinity of the plasma–liquid interface. This technology would be more applicable to large-scale treatment processes if the plasma volume and the plasma–liquid surface area could be dramatically increased. The DMPR, in addition to being a batch treatment process, is not inherently scalable. It also does not utilize the advantage associated with plasma treatment at atmospheric pressure, that is, the ability to continuously treat liquid. In the present work, a kinetic analysis of the data from the oxidation experiments discussed previously (Johnson et al., 2003; Manolache et al., 2004), together with energy distribution data, are used to develop a tubular high-density plasma reactor capable of continuously treating contaminated liquid feeds at high rates.

2. Experimental methods

Interphase mass transfer and energy consumption experiments were carried out independently using the DMPR. A schematic of the reactor, showing the two configurations used in the experiments conducted by Johnson et al. (2003), is shown in Fig. 1. The major components of the DMPR include a reaction vessel containing a rotating upper pin electrode array, a stationary lower electrode, cooling system, and gas introduction and discharge ports. The reactor was equipped with a cooling jacket that allowed for control of the system temperature when a plasma discharge was initiated. A more detailed description of the reactor can be found in Manolache et al. (2001, 2004).

For the interphase mass transfer experiments, 250 mL solutions containing either 50 ppm MTBE or 20 ppm benzene where charged to the DMPR. Oxygen was bubbled through the middle of the stationary electrode at 400 mL/min and was not recirculated. The electrode gap between the pin tips and the lower, stationary electrode was 500 μm, and the upper pin array was spun at 1000 rpm. MTBE (⩾99.8% purity) and benzene (99.6% purity) were obtained from Aldrich Chemical Co. Millipore water was generated by a Milli-Q ultrapure water system and was used as the solvent phase. The analytical techniques and procedures used to quantify MTBE and benzene are described in Johnson et al. (2003).

For experiments focused on energy distributions, the DMPR was charged with 250 mL of millipore water. Again, the electrode gap was 500 μm and the upper pin electrode array was spun at 1000 rpm. Tap water, at a temperature of approximately 295 K, was flushed through the jacket at 1.17 ± 0.04 L/min. The temperature of the bulk liquid was recorded by an Orion 550A temperature and conductivity meter, as shown in Fig. 1, at 30 s intervals and transmitted to LabWorks® via a RS-232 serial connection. The energy transferred to the body of the reactor, recirculation loops and pumps was found to have a negligible effect on the bulk liquid temperature for the time scale of the experiments. Data for the oxidation experiments were taken from Johnson et al. (2003) and Manolache et al. (2004).

3. Results and discussion

Initial experiments conducted with the DMPR provided data associated with the energy distribution and the interphase mass transfer of benzene and MTBE from the liquid to the gas phase within the reactor. An energy balance on the DMPR was carried out to quantify the energy transferred into the bulk liquid from the plasma discharge in the form of sensible heat. The rate of change of the bulk liquid temperature is equal to the heat generation rate of the plasma discharge and the rate of heat loss to the cooling jacket. This energy balance statement can be written as

$$\left(\frac{dT}{dt}\right)_{\text{Reactor}} = \left[\frac{\dot{g}_{\text{exp}}}{\rho C_p} - \left(\frac{dT}{dt}\right)_{\text{Cooling jacket}}\right], \quad (1)$$

where $\dot{g}_{\text{exp}}$ is the plasma power density, ρ is the liquid density, and C_p is the liquid heat capacity. The density and heat capacity of the liquid were assumed to be constant and that of 30 °C water, with values of 996 kg/cm^3 and 4178 J/(kg K) (Cengel, 1998), respectively.

Three experiments were performed to determine the rate of change of the bulk liquid temperature and the rate of heat transfer to the cooling jacket. The results are shown in Fig. 2. Calculated values for the rate of change of the bulk liquid temperature at times $t = 10$ and 11 min were determined using the experimental data and are listed in Table 1. Once the plasma was extinguished, the rate of energy loss to the

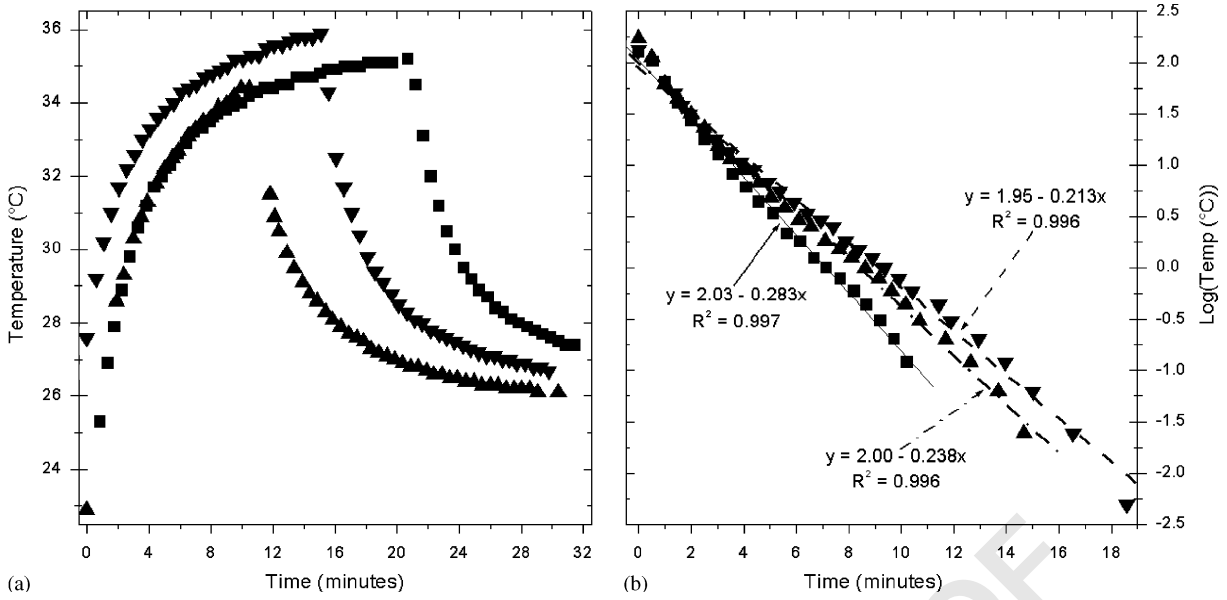

Figure 2 – (a) Plots of the bulk liquid temperature in the DMPR as a function of time during energy distribution experiments and the dissipation of energy to the cooling jacket when the plasma was deactivated. (b) Semi-log plots of the reactor fluid temperature verses time for three aqueous DMPR experiments due to heat loss to the cooling jacket as well as the linear fit used to determine the rate of energy loss.

Table 1 – Computed values for the rate of change of the bulk liquid temperature and the plasma power density, $\dot{g}_{exp}$, at times t = 10 and 11 min

Bulk liquid increase in temperature	10 min (K/min)	11 min (K/min)	Rate of energy loss to cooling jacket		$\dot{g}_{exp}$ (kW/cm^3) 10 min	11 min
$\left(\frac{\Delta T}{\Delta t}\right)_1$	1.16	1.08	$\left(\frac{d(\log T)}{dt}\right)_1$	−0.283	30.8	29.0
$\left(\frac{\Delta T}{\Delta t}\right)_2$	0.754	0.703	$\left(\frac{d(\log T)}{dt}\right)_2$	−0.238	5.8	5.6
$\left(\frac{\Delta T}{\Delta t}\right)_3$	1.14	1.06	$\left(\frac{d(\log T)}{dt}\right)_3$	−0.213	36.1	33.5
$\left(\frac{\Delta T}{\Delta t}\right)_{avg}$	1.02	0.945	$\left(\frac{d(\log T)}{dt}\right)_{avg}$	−0.239	24.2	22.7

cooling jacket decayed exponentially. Semi-log plots of temperature verses time, along with linear fits, are also shown in Fig. 2. The corresponding changes in log(*T*) with time, which were used to calculate the rate of energy dissipation to the cooling jacket, are also listed in Table 1. The plasma power density, displayed in Table 1 for each experiment, is subsequently determined using the calculated energy transfer rates to both the reactor and the cooling jacket, in conjunction with Eq. (1). It was found from experimental data that the average *plasma* power density was 23.5 kW/cm^3. To calculate an estimate of the *applied* plasma power density, $\dot{g}_{calc}$, it is assumed that the input power is constant. Then, for an applied power $\dot{G} = 200$ W, $\dot{g}_{calc} = \dot{G}/V_{plasma} \approx 645$ kW/cm^3 when the plasma volume generated at each pin electrode is 3.1×10^{-4} cm^3. This predicted value is significantly greater than the 23.5 kW/cm^3 obtained from the experiments. As a result, it is estimated that approximately 4% was transferred into the bulk liquid as sensible heat.

Interphase mass transfer data obtained from these experiments and Manolache et al. (2004) are combined with modified Raoult's law to calculate the equilibrium ratios for each organic molecule—MTBE and the BTEXs—solvated in water. Modified Raoult's law may be written as $K_i = \gamma_i P_i^s/P$ and is applicable to non-ideal liquid solutions at near-ambient pressures. The equilibrium ratio, $K_i = y_i/x_i$, is the ratio of mole fractions of a species present in the vapor and liquid phase. The activity coefficients (γ_i) are calculated by first estimating the infinite dilution activity coefficients (γ_i^∞), calculating the van Laar coefficients ($A_{i,\,H_2O}$ and $A_{H_2O,\,i}$), and then using the van Laar equations with the appropriate experimental data to calculate the activity coefficients, $\gamma_i(x_i)$ and $\gamma_{H_2O}(x_i)$ (Seader and Henley, 1998; Walas, 1985; Turner et al., 1996). This approximation is valid for solvent activity coefficients near unity and relatively low solubilities (Turner et al., 1996), making this approach applicable. The *K*-values for MTBE and the BTEXs are calculated using modified Raoult's law with activity coefficients calculated from the van Laar equations. The vapor pressures (P_i^s) and activity coefficients, along with

Table 2 – Selected physical properties as well as calculated values needed to determine the binary system equilibrium ratio of MTBE, benzene, ethylbenzene, toluene, *m*- and *p*-xylene, and *o*-xylene solvated in water (Turner et al., 1996; Burdick and Jackson, 2002)

Properties	MTBE	Benzene	Ethyl-benzene	Toluene	*m*- and *p*-xylene	*o*-xylene
Solubility in water (mole %)	4.8	0.041	0.0029	0.010	0.0030	0.0030
Solubility of water (mole %)	1.5	0.302	0.256	0.257	0.267	0.261
P_i^s (atm)	0.316	0.124	0.0125	0.0371	$8.69 \times 10{-}3$	8.69×10^{-3}
Calculated values	MTBE	Benzene	Ethyl-benzene	Toluene	*m*- and *p*-xylene	*o*-xylene
γ_i^∞	20.83	2466	34,898	9604	33,134	33,134
$\gamma_{H_2O}^\infty$	66.67	331	391	389	375	383
A_{i,H_2O}	3.036	7.81	10.5	9.17	10.4	10.4
$A_{H_2O,i}$	4.200	5.80	5.97	5.96	5.93	5.95
γ_i	20.82	2455	34550	9550	32,100	32,675
K-value	6.57	305	433	354	279	384

calculated *K*-values for MTBE and the BTEXs are listed in Table 2. The *K*-values for the aromatic compounds are approximately 50 times that of MTBE, indicating that the aromatic compounds are transferred from the liquid phase to the gas phase much more readily than MTBE for the experimental conditions used in the DMPR. This is not surprising since the vapor pressures of the BTEXs are higher than that of MTBE. This result is advantageous because, as shown below during the development of the tubular high-density plasma reactor, the rate of plasma-initiated oxidation is enhanced by higher interphase mass transfer coefficients.

4. Tubular high-density plasma reactor

As discussed above, the DMPR was used to treat water artificially contaminated with MTBE and BTEX. Although the DMPR has been shown to be a promising tool for the treatment of organically contaminated aqueous solutions, the original design is not robust, presents scale-up difficulties, and has a high capital cost. Data from previous experiments performed by Johnson et al. (2003) and Manolache et al. (2004), along with a species balance have been used to identify the dimensions and operating conditions for a prototype tubular high-density plasma reactor.

The tubular high-density plasma reactor, shown in Fig. 3, contains an inner stationary shaft (through which a gas is introduced into the system), a middle rotating cylinder (to which the pin electrodes are attached), and an outer stationary cylinder. Contaminated water is continuously fed into the top of the reactor through ports on the outer stationary cylinder and travels axially through the gap between the outer cylinder and the middle rotating cylinder either by a pressure gradient or gravimetric forces. Pin electrodes, represented by black dots, protrude outward from the middle cylinder and are arranged in a helical pattern. For the following analysis, it is important to note that the electrode gap, or distance between the pin tips and the outer stationary cylinder, is virtually identical to the distance between the middle rotating cylinder and the outer cylinder.

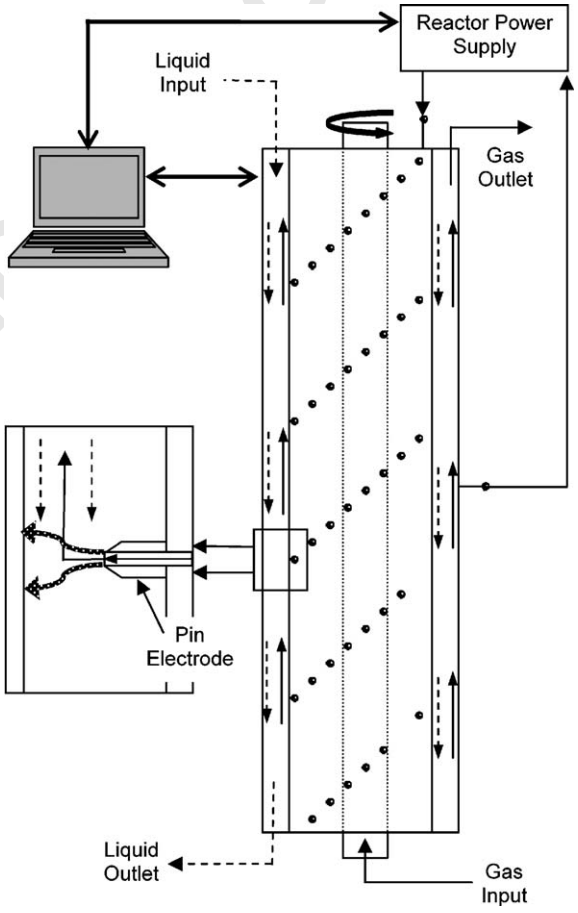

Figure 3 – A schematic of a prototype tubular high-density plasma reactor. Gas (——▶) and liquid (– – – – ▶) flow patterns are shown as well as the possible plasma discharge path from the pin electrodes to the cylindrical electrode through the passing fluid, which is a combination of the gas introduced through the middle of the pin electrodes and the liquid flowing through the annulus. *Note*: lengths are not to scale.

Table 3 – Rate constants for the removal of MTBE, benzene, ethylbenzene, toluene, *m*- and *p*- xylene, and *o*-xylene in a DMPR along with diffusion coefficients used to calculate specie profiles in conjunction with the mass balance

	MTBE	Benzene	Ethyl-benzene	Toluene	*m*- and *p*-xylene	*o*-xylene
k_{rxn} (s^{-1})	0.003	0.172	0.172	0.172	0.172	0.172
k_{mt} ($ppm^{-1}\,s^{-1}$)	1.40×10^{-6}	3.70×10^{-5}	5.13×10^{-5}	5.47×10^{-5}	1.26×10^{-5}	2.70×10^{-5}
k_p ($ppm\,s^{-1}$)	0	0	0	0	0	0
D_{i,H_2O} (cm^2/s)	1.04×10^{-5}	1.14×10^{-5}	9.31×10^{-4}	1.02×10^{-5}	9.31×10^{-4}	9.31×10^{-4}

Once the gas is introduced into the bulk solution, through small holes in the center of each pin electrode, it travels axially with the aqueous solution and is released through a valve at the top of the reactor. When a potential is applied to the middle cylinder, a discharge is initiated at the tips of the pin electrodes that propagates radially to the outer cylinder.

Four rate processes must be considered when performing a mass balance on a chemical species in the tubular high-density plasma reactor—accumulation, convective mass transfer, diffusion, and sources and/or sinks due to physical and chemical mechanisms. The dimensional form of the species conservation equation is

$$\frac{\partial C_i}{\partial t} + \underline{v}\,\nabla C_i = D_{i_{mix}} \nabla^2 C_i + r_i, \tag{2}$$

where $\underline{v}$ is the local velocity vector, $D_{i_{mix}}$ is the diffusion coefficient for species i in the mixture, and r_i is the net production rate of species i (which in this case is negative) by a series of homogeneous reactions. Concentration profiles for MTBE and the BTEXs are developed for the tubular reactor when operating under batch and steady flow conditions.

4.1. *Batch operation*

To compare the ability of the tubular high-density plasma reactor to treat organically contaminated aqueous solutions with that of the DMPR, concentration profiles for batch operation have been developed. When operated in a batch configuration, the tubular reactor has virtually no axial, angular, or radial concentration gradients because the plasma discharge is, in effect, uniform throughout the reactor. The species conservation equation thus reduces to the following ideal batch reactor design equation:

$$\frac{\partial C_i}{\partial t} = r_i. \tag{3}$$

To evaluate the production rate of species i, three loss processes are considered when removing a volatile organic compound from an aqueous solution in the reactor: oxidation due to the plasma, interphase mass transfer and photolysis. These loss processes can be expressed as

$$r_i = \frac{\ln a}{\alpha} C_{i_0} \exp\left(\frac{\ln a}{\alpha} t\right) + \left(\frac{A_I}{V_g} D_{i_{mix}} \nabla y_i\right) C_i + \phi(\lambda) I_0(\lambda, t)[1 - \exp(-2.303 \varepsilon L C_i)]. \tag{4}$$

The first term describes the loss of species i due to the plasma, where a is the volume fraction of fluid not in the plasma state, α is a time constant associated with the discharge characteristics of the reactor and has a value of 1 ms, t is time, and C_{i_0} is the initial concentration of species i (Willberg et al., 1996). The second term describes the loss of species i through interphase mass transfer (Johnson et al., 2003), and the third due to photolysis (Sun et al., 2000). However, Eq. (4) can be rearranged, and further simplified, yielding

$$\frac{dC_i}{dt} = -k_{rxn} C_i - k_{mt} C_i^2 - k_p, \tag{5}$$

where k_{rxn} is a first-order rate constant associated with degradation due to the plasma, k_{mt} is a second-order interphase mass transfer rate constant, and k_p is a zero-order photolysis rate constant. A combination of non-linear least-squares analysis and MATLAB® optimization techniques were used to determine the rate constants, which are listed in Table 3 for each species. Predicted concentration profiles for the loss of each species due to interphase mass transfer and the plasma, as well as the non-linear least-squares fit to experimental data from Johnson et al. (2003) and Manolache et al. (2004) for the combination of the two processes are plotted in Fig. 4.

The concentration at any point in the fluid can be determined by solving Eq. (5) and is

$$C_i = \frac{z \exp(xt + y) + k_{rxn} + x}{2k_{mt}(\exp(xt + y) - 1)}, \tag{6}$$

where $x = \sqrt{(-k_{rxn})^2 - 4k_{mt}k_p}$, $y = \log[(-2k_{mt}C_{i_0} - k_{rxn} - x)/(-2k_{mt}C_{i_0} - k_{rxn} + x)]$ and $z = x - k_{rxn}$. The first-order rate constant, k_{rxn}, is a function of the plasma volume, which is estimated to be a linear function of the electrode gap and number of pin electrodes (Roth, 1995). Concentration profiles developed using the rate constants in Table 3, and accounting for changes in the electrode gap and number of pin electrodes, demonstrate that the tubular high-density plasma reactor has the ability to efficiently remove volatile organic compounds from aqueous solutions. Figure 5 contains predicted values of normalized species concentrations as a function of treatment time for varying electrode gaps and number of pin electrodes.

When a tubular reactor with 500 pin electrodes is configured with an electrode gap of 500 μm, a treatment time of approximately 2.2 min is required to reduce the MTBE—the most difficult to remove of the species considered—concentration below the recommended drinking water standard of approximately 20 ppb (USEPA, 2002). The remaining BTEX concentrations are more readily removed from solution, and thus meet drinking water standards at lower treatment times. The predicted time needed to reduce each species concentra-

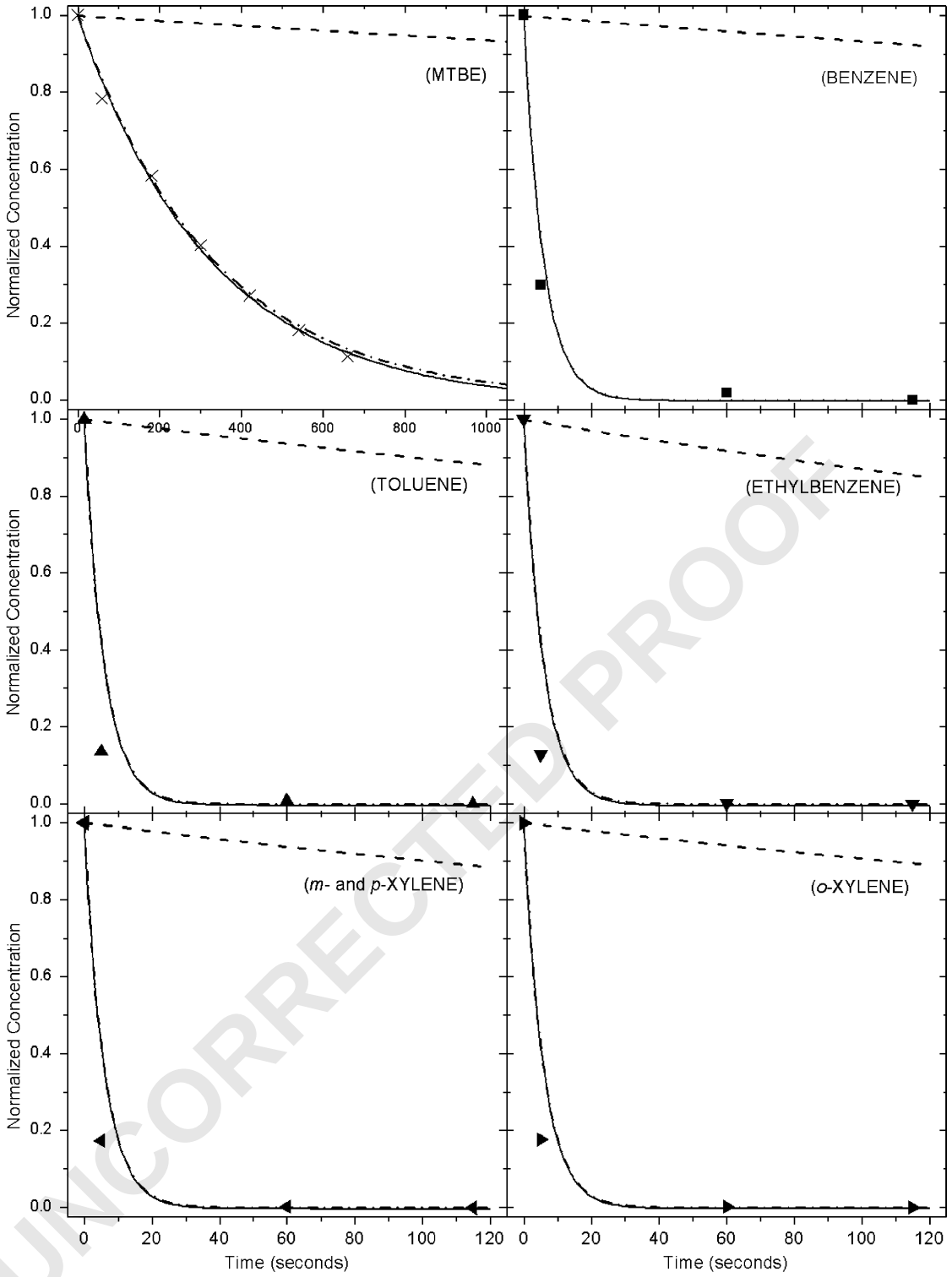

Figure 4 – Plots of the normalized species concentration versus time for the removal of MTBE (×), benzene (■), toluene (▲), ethylbenzene (▼), *m*- and *p*-xylene (◀) and *o*-xylene (▶) in a DMPR (Johnson et al., 2003; Manolache et al., 2004), as well as the curves describing losses due to sparging (– – –), the plasma (– · –) and the combined effects of the discharge (—). Notice that for the BTEXs, the plasma curve and combined effects curve are almost indistinguishable.

tion below the drinking water standard for different reactor configurations is shown in Table 4. A reasonable dimension for a reactor housing 500 pin electrodes is 150 cm (5 ft) in length and 7.6 cm (3 in) in diameter. Using these dimensions and an electrode gap of 500 μm, it is estimated that the treatment volume is 180 mL. One route to larger treatment volumes is to increase the electrode gap, provided the plasma discharge can be sustained. For example, the same reactor

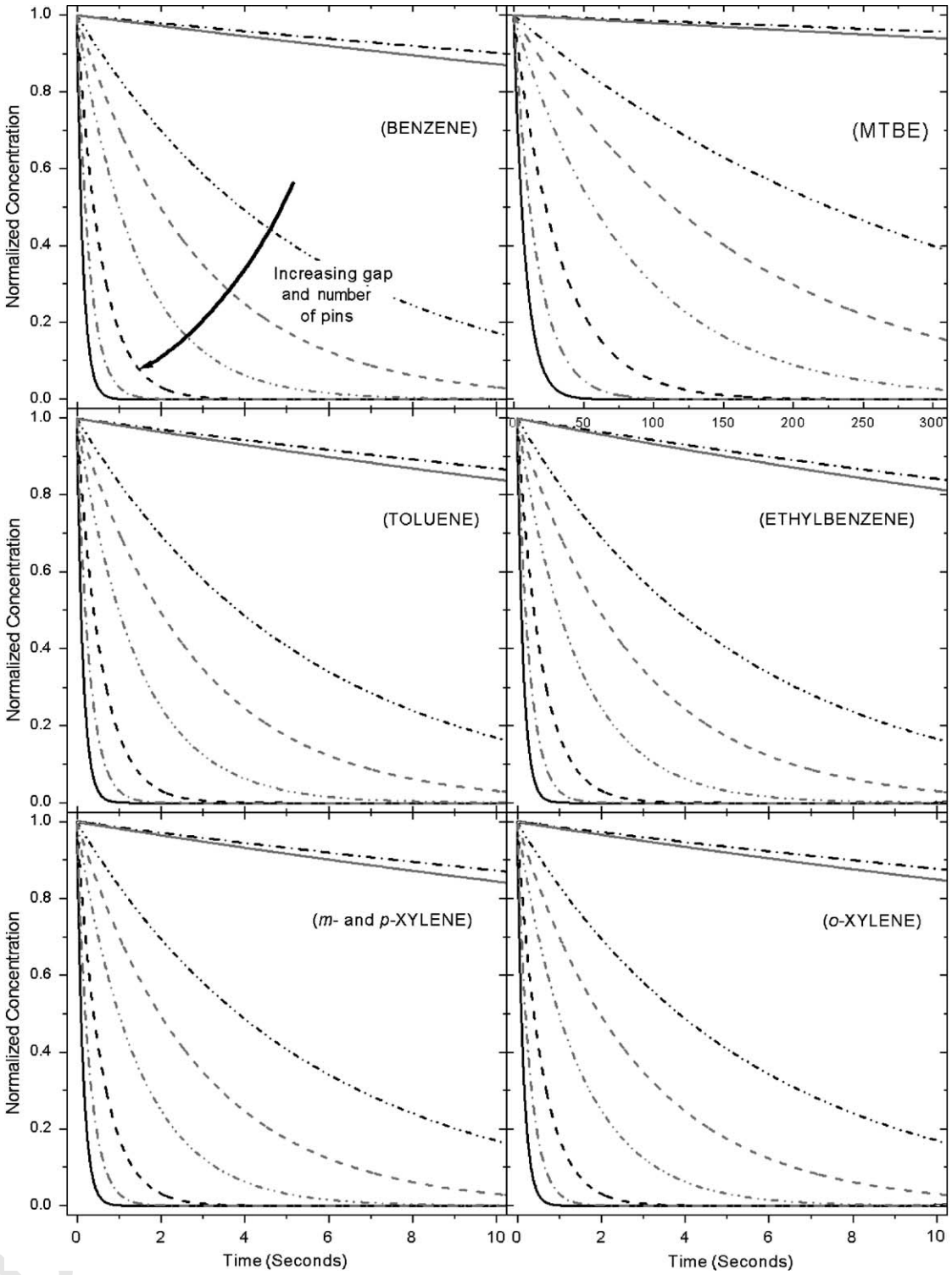

Figure 5 – Plots of the predicted normalized concentration profiles for the removal of benzene, MTBE, toluene, ethylbenzene, *m*- and *p*-xylene and *o*-xylene from an aqueous solution versus treatment time in a tubular high-density plasma reactor operated under batch conditions for varying electrode gaps and number of pin electrodes. Black curves correspond to 25 pin electrodes and electrode gaps of 0.001 cm (— · –), 0.05 cm (— · · —), 0.5 cm (– –) and 2 cm (—). Gray curves correspond to an electrode gap of 0.05 cm and 1 pin electrode (——), 50 pin electrodes (— —), 100 pin electrodes (—— · ——) and 500 pin electrodes (—— · ——).

Table 4 – Treatment time and corresponding concentration for the removal of MTBE, benzene, ethylbenzene, toluene, *m*- and *p*- xylene, and *o*-xylene in a batch tubular high-density plasma reactor as well as volumetric flow rate and exit concentration for a tubular reactor with a continuous feed for varying electrode gaps and number of pin electrodes

	MTBE	Benzene	Toluene	Ethylbenzene	*m*- and *p*-xylene	*o*-xylene
♯ of pins Electrode gap	Time (s) Conc. (ppb)	Time (s) Conc. (ppb)	Time (s) Conc. (ppb)	Time (s) Conc. (ppb)	Time (s) Conc. (ppb)	Time (s) Conc. (ppb)
Batch configuration						
25 pins	1.2×10^{5}	2.7×10^{3}	1.2×10^{3}	1.3×10^{3}	8.9×10^{2}	6.8×10^{2}
0.001 cm	20	5.0	10	7.0	10	10
25 pins	2.6×10^{3}	61	31	34	26	21
0.05 cm	20	5.0	10	6.9	9.9	10
25 pins	2.6×10^{2}	6.2	3.1	3.5	2.6	2.1
0.5 cm	19	4.5	10	7.0	10	10
25 pins	6.6×10^{1}	1.5	0.78	0.87	0.65	0.53
2 cm	19	5.0	10	7.0	9.9	9.9
1 pin	6.1×10^{4}	1.4×10^{3}	6.4×10^{2}	7.0×10^{2}	5.1×10^{2}	4.0×10^{2}
0.05 cm	20	5.0	10	7.0	10	10
50 pins	1.3×10^{3}	31	16	17	13	11
0.05 cm	20	4.9	10	7.0	9.9	9.9
100 pins	6.5×10^{2}	15	7.9	8.7	6.5	5.3
0.05 cm	20	4.8	9.4	6.7	9.7	9.7
500 pins	1.3×10^{2}	3.1	1.6	1.7	1.3	1.1
0.05 cm	18	5.0	10	7.0	10	10
500 pins	3.3	7.7×10^{-2}	4.0×10^{-2}	4.4×10^{-2}	3.3×10^{-2}	2.7×10^{-2}
2 cm	18	4.9	9.0	6.4	9.2	9.2
♯ of pins Electrode gap	Q (L/min) Conc. (ppb)	Q (L/min) Conc. (ppb)	Q (L/min) Conc. (ppb)	Q (L/min) Conc. (ppb)	Q (L/min) Conc. (ppb)	Q (L/min) Conc. (ppb)
Continuous flow configuration						
25 pins	2.2×10^{-11}	9.6×10^{-10}	2.3×10^{-9}	2.1×10^{-9}	3.0×10^{-9}	3.9×10^{-9}
0.001 cm	18	4.6	960	620	9700	9900
25 pins	2.6×10^{-6}	1.1×10^{-4}	2.2×10^{-4}	2.0×10^{-4}	2.6×10^{-4}	3.2×10^{-4}
0.05 cm	20	5.0	100	700	10,000	9300
25 pins	2.6×10^{-3}	1.1×10^{-1}	2.1×10^{-1}	1.9×10^{-1}	2.6×10^{-1}	3.2×10^{-1}
0.5 cm	20	4.5	960	700	9900	9800
25 pins	1.6×10^{-1}	6.9	14	12	16	20
2 cm	20	4.9	100	640	9500	9900
50 pins	1.2×10^{-5}	4.8×10^{-4}	9.5×10^{-4}	8.7×10^{-4}	1.2×10^{-3}	1.4×10^{-3}
0.05 cm	20	4.2	900	690	9300	9800
100 pins	4.1×10^{-5}	1.7×10^{-3}	3.4×10^{-3}	3.1×10^{-3}	4.1×10^{-3}	5.1×10^{-3}
0.05 cm	20	4.5	990	680	10,000	10,000
500 pins	5.0×10^{-3}	2.2×10^{-1}	4.3×10^{-1}	3.8×10^{-1}	5.2×10^{-1}	6.3×10^{-1}
0.05 cm	17	4.9	990	690	10,000	10,000
500pins	330	14,000	27,000	25,000	33,000	41,000
2 cm	20	5.0	100	700	10,000	10,000

configured with an electrode gap of 2 cm would reduce the time to degrade MTBE to 3.3 s while also treating approximately 5.4 L of contaminated liquid. Supplementary Fig. S1 contains two contour plots for the removal of MTBE and ethylbenzene as a function of the number of pin electrodes and electrode gap for 3.3 s of treatment. It is clearly shown that increasing the number of pins and the electrode gap will reduce the time required for treatment. It is also apparent when comparing the MTBE contour plot with that of ethylbenzene, a species with a higher *K*-value will be removed from solution at a faster rate. The higher volatility of the aromatic compounds more readily promotes them to the plasma state where electron dissociation reactions occur, thus increasing the removal rate. Although operating the tubular high-density plasma reactor in a batch configuration may be a viable treatment option for organically contaminated aqueous solutions, the system is more effective operating under continuous flow conditions when targeting scale-up and throughput issues.

4.2. *Continuous flow operation*

To determine the effectiveness of the tubular reactor in its intended operational configuration, concentration profiles for MTBE and the BTEXs are developed for continuous flow. Under steady-state conditions, the first term in Eq. (2) vanishes and further simplifications may be possible, depending on the relative magnitudes of the convection and diffusion terms. To investigate this, the species equation is written in dimensionless form. Rewriting each term with a

dimensionless concentration, $\varphi_i = C_i/C_{i_0}$, and its corresponding dimensional scaling factor, the dimensionless form of the equation is

$$Pe_i\left(\frac{d\varphi_i}{dz}\right) = \frac{d^2\varphi_i}{dz^2} + \sum_{ij} Da_{ij} r^*_{ij}, \quad (7)$$

where $Pe_i = Lv_{avg}/D_{i_{mix}}$, $Da_{ij} = k_{ij}L^2C_{i_0}^{n-1}/D_{i_{mix}}$, L is the length of the reactor and $r^*_{ij} = r_{ij}/(k_{ij}C^n_{i_0})$. The tubular high-density plasma reactor has a continuous input and an impermeable outer wall. Thus, the local velocity vector is replaced with a scalar cross-sectional average velocity and is contained in the mass transfer Peclet number, *Pe*. The mass transfer Peclet number relates the rate of convective mass transfer to the rate of diffusion. When $Pe \gg 1$, as is typical in a liquid, the diffusion term in Eq. (7) may be neglected if the Damköhler number, *Da*, is also large, resulting in the classic plug flow equation. Therefore, it is important to consider whether the system is mass transfer limited by evaluating *Da*. The Damköhler number relates the rate of reaction of species *i* to the rate of transport of species *i* through the reaction zone. Using the empirical Wilke–Chang equation (Wilke and Chang, 1955) to calculate $D_{i_{mix}}$, (Table 3), it was found that $Da \gg 1$ for all species and operating conditions; thus, the rate of diffusion is extremely small relative to the reaction rate.

When neglecting diffusion and using the expression for r_i developed previously, the dimensionless species balance can be further reduced and expressed as

$$\frac{d\varphi_i}{d\zeta} = -\frac{L^2}{v_{avg}}\left(k_{rxn}\varphi_i + k_{mt}C_{i_0}\varphi_i^2 + \frac{k_p}{C_{i_0}}\right), \quad (8)$$

where $\zeta = z/L$ is the dimensionless reactor length. Thus, the normalized concentration of species *i* as a function of axial position is

$$\varphi_i = \frac{z\exp(y - xL\tau\zeta) - k_{rxn} + x}{2k_{mt}C_{i_0}(1 - \exp(y - xL\tau\zeta))}, \quad (9)$$

where $x = \sqrt{k^2_{rxn} - 4k_{mt}k_p}$, $y = \log[(2k_{mt}C_{i_0} + k_{rxn} - x)/(2k_{mt}C_{i_0} + k_{rxn} + x)]$, $z = k_{rxn} + x$ and $\tau = L/v_{avg}$ is the average residence time. As before, the first-order rate constant, k_{rxn}, is a function of the plasma volume, making this quantity directly proportional to the electrode gap and number of pin electrodes. Concentration profiles are again computed using the rate constants in Table 3 while accounting for changes in the electrode gap and number of pin electrodes. Trends in the predicted normalized concentration for all six species as a function of the electrode gap and number of pin electrodes (data not shown) are similar to that found for the batch configuration. The exit concentration, corresponding to a dimensionless length of unity, decreases with an increase in the electrode gap and number of pin electrodes when the inlet fluid velocity and species concentration are fixed.

To compare the different modes of operation, batch and continuous flow, the same design specifications as in the previous section are used in the following calculations. Instead of residence time in the tubular reactor, however, the results are presented as a function of volumetric flow rate. Figure 6 contains calculated normalized concentration profiles for MTBE and the BTEXs versus volumetric flow rate for varying operating conditions. A reactor housing 500 pin electrodes configured with electrode gaps of 0.05 and 2 cm will reduce the MTBE concentration below the recommended drinking water standard at volumetric flow rates of 5.0×10^{-3} and 330 L/min, respectively. The remaining BTEX concentrations are reduced below drinking water standards at higher flow rates. The volumetric flow rates predicted for each species for various reactor configurations are listed in Table 4.

5. Summary

A tubular high-density plasma reactor may be an effective tool in the removal of volatile organic compounds from aqueous solutions. The new design presented here is easier to scale up for industrial use, especially when operated under continuous flow conditions. The prototype reactor also reduces the sputtering rate, i.e., the wear of the electrodes when compared to other point-to-plane reactors. This is accomplished by incorporating a large number of pins in parallel, thereby reducing the current density at each pin tip, which controls the sputtering rate, while still applying the same voltage drop across the electrode gap. Although rate constants for the removal of volatile organics have been determined for only six compounds, the removal rate constant for a given species, voltage, current, electrode gap, gas composition, and gas flow rate should be higher than that of MTBE if its *K*-value is also higher. If MTBE is used as a surrogate molecule for contaminated water, a configuration of eight reactors, each 5 ft in length configured with an electrode gap of 2 cm and 500 pin electrodes, has the potential to treat 1 MGD of contaminated liquid. However, MTBE has a vapor pressure higher than most contaminants in wastewater streams. Thus, to ascertain the volumetric flow rate needed to treat waste streams more representative of what is produced industrially, it is important to determine the rate constants associated with the treatment of water contaminated with species having a *K*-value of approximately zero.

The tubular plasma reactor is also designed to maximize the time in which a fluid element moving axially through the reactor is in contact with the plasma. This is accomplished by minimizing the distance that the pin electrodes protrude from the rotating cylinder. Because of this design implementation, the fraction of fluid in the annular gap contacting the plasma is maximized, a significant improvement over the initial DMPR design, whereby a significant fraction of the fluid—approximately 90%—bypasses the plasma as it moves through the reaction zone. As a result, the first-order rate constant associated with the plasma will be higher in the tubular reactor, so that the results displayed in Table 4 may be viewed as upper limits. Also, the zero-order rate constant associated with photolysis may not be negligible in the tubular reactor, particularly when 500 pin electrodes are employed, 20 times more than in the DMPR configuration. Thus, the rate constants used in this study to predict the effectiveness of the prototype reactor are conservative, and experiments conducted on the tubular reactor should yield lower treatment times and higher volumetric flow rates.

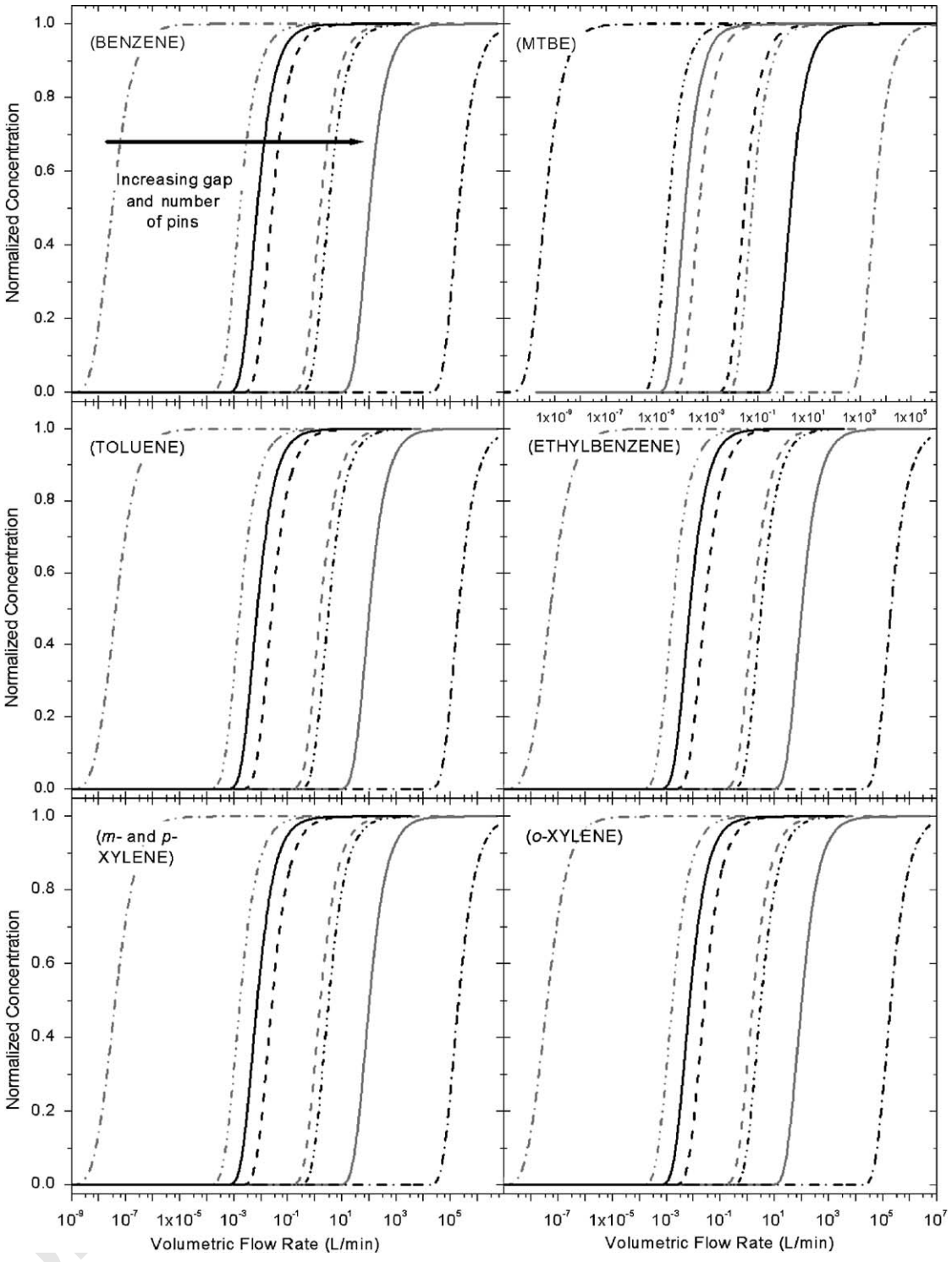

Figure 6 – Plots of the calculated normalized concentration profiles for the removal of benzene, MTBE, toluene, ethylbenzene, *m*- and *p*-xylene and *o*-xylene from an aqueous solution versus volumetric flow rate in a tubular high-density plasma reactor operated under continuous feed conditions for varying electrode gaps and number of pin electrodes. Gray curves correspond to 25 pin electrodes and electrode gaps of 0.001 cm (— · —), 0.05 cm (— · · —), 0.5 cm (– –) and 2 cm (——). Black curves correspond to an electrode gap of 0.05 cm and 50 pin electrodes (—), 100 pin electrodes (– –), 500 pin electrodes (— · · —), and an electrode gap of 2 cm with 500 pin electrodes (— · —).

Acknowledgments

This work was support by the National Institutes of Health, Grant Number EB00726; the Office of Naval Research, Grant Number N00014-00-WX2-1163; and the National Science Foundation's Fast Track to Work Scholarship Program.

Appendix A. Supplementary materials

Supplementary data associated with this article can be found in the online version at doi:10.1016/j.watres.2005.11.015.

REFERENCES

Burdick and Jackson, 2002. Solvent physical properties. http://www.bandj.com/BJSolvents/Solvents/MethyltbutylEther/MtBEther.htm

Cengel, Y.A., 1998. Heat Transfer: A Practical Approach. WCB, McGraw-Hill, Boston, MA.

Denes, F.S., Young, R.A., 1996. Apparatus for reactions in dense-medium plasmas. US patent #5,534,232.

Johnson, D.C., Shamamian, V.A., Callahan, J.H., Denes, F.S., Manolache, S.O., Dandy, D.S., 2003. Treatment of methyl *tert*-butyl ether contaminated water using a dense medium plasma reactor: a mechanistic and kinetic investigation. Environ. Sci. Technol. 37, 4804–4810.

Manolache, S., Somers, E.B., Wong, A.C.L., Shamamian, V., Denes, F., 2001. Dense medium plasma environments: a new approach for the disinfection of water. Environ. Sci. Technol. 35, 3780–3785.

Manolache, S.O., Shamamian, V.A., Denes, F., 2004. Dense medium plasma–plasma-enhanced decontamination of water of aromatic compounds. J. Environ. Eng. 130, 17–25.

Roth, J.R., 1995. Industrial Plasma Engineering, vol. 1: Principles. Institute of Physics Publishing, Philadelphia, PA.

Seader, J.D., Henley, E.J., 1998. Separation Process Principles. Wiley, New York.

Sun, B., Sato, M., Clements, J.S., 2000. Oxidative processes occurring when pulsed high voltage discharges degrade phenol in aqueous solution. Environ. Sci. Technol. 34, 509–513.

Turner, L.H., Chiew, Y.C., Ahlert, R.C., Kosson, D.S., 1996. Measuring vapor–liquid equilibrium for aqueous-organic systems: review and a new technique. AIChE J. 42, 1772–1788.

USEPA, 2002. MTBE in drinking water. http://www.epa.gov/safewater/mtbe.html

Walas, S.M., 1985. Phase Equilibria in Chemical Engineering. Butterworth, Boston, MA.

Wilke, C.R., Chang, P., 1955. Correlation of diffusion coefficients in dilute solutions. AIChE J. 1, 264–270.

Willberg, D.M., Lang, P.S., Hochemer, R.H., Kratel, A.W., Hoffmann, M.R., 1996. Electrohydraulic destruction of hazardous wastes. CHEMTECH 26, 52–57.